This article has been accepted for publication in a future issue of this journal, but has not been fully edited. Content may change prior to final publication. Citation information: DOI 10.1109/TVT.2018.2885555, IEEE Transactions on Vehicular Technology

Analysis of Analog and Digital MRC for Distributed and Centralized MU-MIMO Systems

Shuang Li, *Student Member, IEEE,* Peter Smith, *Fellow, IEEE,*
Pawel Dmochowski, *Senior Member, IEEE,* and Jingwei Yin, *Member, IEEE*

***Abstract*—We present analytical expressions for the expected per-user signal power and interference in a multi-user multiple input multiple output system with analog maximal ratio combining (MRC) on the uplink and with matched filtering (MF) precoding on the downlink. This leads to a closed-form approximation of expected per-user signal to interference-plus-noise ratio (SINR). The analysis is carried out for different base station layouts, including a centralized collocated array and a distributed system with arbitrarily correlated Rayleigh fading. Unlike the digital MRC system, where the performance improves for a more distributed system, we show that analog MRC performs best in a centralized configuration. Furthermore, numerical results show that both analog and digital MRC benefit from a strong line-of-sight (LoS) presence in Ricean fading channels as the Rice K factor reduces the interference power. We show that in a centralized system, the performance of analog and digital MRC converge with increasing K factor, because strong LoS reduces the diversity of incoming signal power utilized by digital MRC. On the other hand, in a distributed system the performance gap between these two techniques will remain due to the diversity of signal powers. Our closed-form approximation of the expected per-user SINR is general and appropriate for moderate to large numbers of antennas and arbitrary correlation models.**

***Index Terms*—Expected SINR, analog MRC, digital MRC, spatial correlation, Rice K factor.**

I. Introduction

Multi-User Multiple Input Multiple Output (MU-MIMO) systems have the ability to serve many users over the same time-frequency resource via various beamforming techniques, significantly improving the spectral efficiency (SE) of wireless communication systems. In order to meet the ever-increasing demand for data rate, emerging MIMO systems are likely to employ a large number of antennas.

Considering hardware costs, a purely analog architecture at the base station (BS) forms an attractive design option. Furthermore, distributed BSs with large antenna arrays are of great interest as they provide the additional benefit of improved coverage [1] and reduction of spatial correlation relative to large collocated arrays [2]. Maximal ratio combining (MRC) not only maximizes the received signal power, but also requires no central control and can be deployed independently at each antenna in a distributed BS layout [2]. In recent years, a number of works have analysed the simplest forms of diversity combining techniques, including MRC, equal-gain combining (EGC) and selection combining (SC). Among these, the work in [3] shows that EGC is of practical interest as it outperforms SC and has a lower complexity compared to digital MRC. In purely analog MIMO systems, MRC is equivalent to EGC as analog processing is not able to change the signal amplitude.

For single-user MIMO, most analytical work concerning analog MRC is conducted from the perspective of modulation, outage probability and bit error probability (BEP) (eg [4] and references within). The performance of digital MRC in a distributed system is analysed in [2]. For uplink MU-MIMO, a thorough performance analysis of digital MRC over Rayleigh fading without spatial correlation effects is presented in [5]. A sum-rate analysis of digital MRC, as well as zero-forcing and minimum mean squared error combing, is presented in [6] for independent Rayleigh fading. Closed-form approximations of SINR and the ergodic sum SE of a MU-MIMO downlink system using digital MRC with correlation are presented in [7]. For a single user MIMO link in correlated Ricean fading, digital MRC at the receiver combined with digital maximum ratio transmission is analysed in [8]. Despite this considerable body of work, research related to analog MRC in Ricean channels is very limited, mainly focusing on system energy efficiency or system sum rate [9], [10] in single-user MIMO systems. Thus, we present numerical results adopting a Ricean fading channel to analyse the system performance in a MU-MIMO system.

To the best of our knowledge, there exist no closed-form SINR results for analog MRC in the uplink and downlink matched filtering (MF) in a correlated Rayleigh fading environment for both centralized and distributed MU-MIMO systems. Hence, to fill this gap, this paper presents a thorough analysis of the expected per-terminal SINR based on different BS layouts and gives insights on the impact of system parameters. Specifically, the contributions of this paper are as follows:

- Novel analytical expressions of expected per-user signal power and interference for both uplink MRC and downlink MF are derived. The derivation is robust to changes in system dimension and correlation models.
- We analyse the system performance of digital and analog

Manuscript received May 4, 2018; accepted November 13, 2018.

S. Li is funded by China Scholarship Council. S. Li and P. A. Dmochowski are with the School of Engineering and Computer Science, Victoria University of Wellington, PO Box 600 Wellington 6140, New Zealand (e-mail: {lishua, pawel.dmochowski}@ecs.vuw.ac.nz).

P. J. Smith is with the School of Mathematics and Statistics, Victoria University of Wellington, PO Box 600 Wellington 6140, New Zealand (e-mail: peter.smith@ecs.vuw.ac.nz).

J. Yin is with the College of Underwater Acoustic Engineering, Harbin Engineering University, Harbin 150001, P.R.China (e-mail: yinjingwei@hrbeu.edu.cn).

MRC/MF for three BS layouts. We show that while digital MRC benefits from increased BS decentralization, the same does not hold for analog MRC.

- Simulation based investigations of the impact of different Rice K factors on both centralized and distributed systems with analog and digital MRC are presented. We show that the performance of analog MRC approaches that of digital MRC when increasing the K factor in a centralized system, while the performance gap between the two technique remains in a distributed system.

II. System Model

Consider a MU-MIMO system with K single antenna users randomly located in a single cell and a total of N_{t} antennas at the BS divided equally amongst M cooperative antenna groups. Three different BS layouts are considered. *Cen* denotes a centralized system where the BS is located at the centre of the cell with all N_{t} antennas; *Dis4* is a distributed system, where antennas are divided equally amongst four cooperative antenna sites with each site (half way from the centre to the cell-edge and 90° from each other) equipped with $\frac{N_{\mathrm{t}}}{4}$ antennas. Similarly, *Dis2* denotes a system with two sites, each (half way from the centre to the cell-edge and 180° from each other) with $\frac{N_{\mathrm{t}}}{2}$ antennas.

A. Uplink System Model

The $N_{\mathrm{t}} \times 1$ channel vector for user i can be written as $\mathbf{h}_i = \mathbf{R}_i^{\frac{1}{2}} \mathbf{u}_i$, where the entries of $\mathbf{u}_i$ are independent and identically distributed (i.i.d) Rayleigh fading variables, $\mathbf{u}_i \sim \mathcal{CN}(\mathbf{0}, \mathbf{I})$; $\mathbf{R}_i$ is the $N_{\mathrm{t}} \times N_{\mathrm{t}}$ spatial correlation matrix for user i. Assuming no correlation between antennas belonging to different groups, we write $\mathbf{R}_i = \text{blkdiag}(\mathbf{R}_{i1}, \mathbf{R}_{i2}, ..., \mathbf{R}_{iM})$, $\mathbf{R}_{im} = \bar{\beta}_{im} \mathbf{\Sigma}_{im}$, where i indicates the user i and m indicates the base station group m. $\mathbf{\Sigma}_{im}$ contains the correlation coefficients and $\bar{\beta}_{im}$ models the effect of pathloss and shadowing of the m^{th} group base station for the i^{th} user. We consider $\bar{\beta}_{im} = A\zeta_{im}(d_0/d_{im})^{\gamma}$, where A is a unit-less constant indicating the geometric attenuation at the reference distance d_0, d_{im} is the distance between the i^{th} user and the m^{th} BS and γ is the pathloss attenuation exponent; ζ_{im} is a log-normal random variable, $10\log_{10}\zeta_{im} \sim \mathcal{N}(0, \sigma_{\text{sh}}^2)$, to model the effect of shadowing between the the i^{th} user and the m^{th} BS. Thus, $\mathbf{H} = [\mathbf{h}_1 \mathbf{h}_2 ... \mathbf{h}_K]$ denotes the $N_{\mathrm{t}} \times K$ fast-fading channel matrix between N_{t} BS antennas and K users. Then, under the assumption of perfect channel knowledge at the BS and equal transmit power for each user, for narrow-band transmission, the received signal at the BS is given by

$$\mathbf{y} = \sqrt{P_{\mathrm{t}}^{\mathrm{ul}}} \mathbf{H}\mathbf{s} + \mathbf{n}_{\mathrm{ul}}, \tag{1}$$

where $\mathbf{s}$ is the $K \times 1$ data symbol vector from the K end users and $\mathbb{E}[\mathbf{s}\mathbf{s}^H] = \mathbf{I}$; $\mathbf{n}_{\mathrm{ul}}$ models the effect of white Gaussian noise, where the noise variance is assumed to be one; $P_{\mathrm{t}}^{\mathrm{ul}}$ is the uplink transmit power per data stream. After MRC processing, the combined signal for the i^{th} user at the BS is given by

$$\mathbf{y}_i = \sqrt{P_{\mathrm{t}}^{\mathrm{ul}}} \mathbf{g}_i^{\mathrm{H}} \mathbf{h}_i s_i + \sqrt{P_{\mathrm{t}}^{\mathrm{ul}}} \sum_{\substack{l=1 \\ l \neq i}}^{K} \mathbf{g}_i^{\mathrm{H}} \mathbf{h}_l s_l + \mathbf{g}_i^{\mathrm{H}} \mathbf{n}_{\mathrm{ul}}, \tag{2}$$

where $\mathbf{g}_i = \mathbf{h}_i$ for digital MRC and $\mathbf{g}_i = \hat{\mathbf{h}}_i$, $\hat{\mathbf{h}}_i = \exp(j\angle\mathbf{h}_i)$ for analog MRC, where $\angle\mathbf{h}_i$ represents the vector of angles of each element of $\mathbf{h}_i$. This results in the SINR given by

$$\text{SINR}_i = \frac{P_{\mathrm{t}}^{\mathrm{ul}} |\mathbf{g}_i^{\mathrm{H}} \mathbf{h}_i|^2}{P_{\mathrm{t}}^{\mathrm{ul}} \left\{ \sum_{\substack{l=1 \\ l \neq i}}^{K} |\mathbf{g}_i^{\mathrm{H}} \mathbf{h}_l|^2 \right\} + \mathbf{g}_i^{\mathrm{H}} \mathbf{g}_i}. \tag{3}$$

B. Downlink System Model

The $K \times N_{\mathrm{t}}$ fast-fading channel matrix for the downlink can be written as $\mathbf{H} = [\mathbf{h}_1^{\mathrm{T}} \mathbf{h}_2^{\mathrm{T}} ... \mathbf{h}_K^{\mathrm{T}}]^{\mathrm{T}}$, where the $1 \times N_{\mathrm{t}}$ channel vector for the i^{th} user is $\mathbf{h}_i = \mathbf{u}_i \mathbf{R}_i^{\frac{1}{2}}$, and $\mathbf{u}_i$ and $\mathbf{R}_i$ are defined in Section II-A with the exception that $\mathbf{u}_i$ is now $1 \times N_{\mathrm{t}}$. The received signal at the i^{th} user can be expressed as

$$\mathbf{y}_i = \sqrt{P_{\mathrm{t}}^{\mathrm{dl}}} \mathbf{h}_i \mathbf{g}_i^{\mathrm{H}} s_i + \sqrt{P_{\mathrm{t}}^{\mathrm{dl}}} \sum_{\substack{l=1 \\ l \neq i}}^{K} \mathbf{h}_i \mathbf{g}_l^{\mathrm{H}} s_l + n_{\mathrm{dl}}, \tag{4}$$

where $P_{\mathrm{t}}^{\mathrm{dl}}$ is the downlink transmit power per data stream, n_{dl} models the effect of white Gaussian noise with unit variance, and $\mathbf{g}_i = \frac{\mathbf{h}_i}{||\mathbf{h}_i||}$ for digital MRC and $\mathbf{g}_i = \frac{\hat{\mathbf{h}}_i}{\sqrt{N_{\mathrm{t}}}}$ for analog MRC. Thus, the corresponding SINR is given by

$$\text{SINR}_i = \frac{P_{\mathrm{t}}^{\mathrm{dl}} |\mathbf{h}_i \mathbf{g}_i^{\mathrm{H}}|^2}{P_{\mathrm{t}}^{\mathrm{dl}} \left\{ \sum_{\substack{l=1 \\ l \neq i}}^{K} |\mathbf{h}_i \mathbf{g}_l^{\mathrm{H}}|^2 \right\} + 1}. \tag{5}$$

III. Approximations of Achievable Uplink and Downlink Spectral Efficiency

In this section, we derive exact closed-form expressions for the expected per-user signal power and interference power for both uplink and downlink analog MRC systems. To enable the analysis, we apply a commonly used approximation as follows: if $X = \sum X_i$ and $Y = \sum Y_i$ are both sums of non-negative random variables, then $\mathbb{E}\left[\log_2\left(1 + \frac{X}{Y}\right)\right] \approx \log_2\left(1 + \frac{\mathbb{E}[X]}{\mathbb{E}[Y]}\right)$ [5]. Independence between X and Y is not required and the result becomes more accurate when the number of the summation terms in X and Y is large [5]. For the uplink system, substituting the analog MRC receive combiner into (3) gives the approximation of per-user spectral efficiency as

$$\mathbb{E}[\mathrm{R}_{\mathrm{ul}}] \approx \log_2 \left\{ 1 + \frac{\frac{P_{\mathrm{t}}^{\mathrm{ul}}}{N_{\mathrm{t}}} \mathbb{E}\left[|\hat{\mathbf{h}}_i^{\mathrm{H}} \mathbf{h}_i|^2\right]}{\frac{P_{\mathrm{t}}^{\mathrm{ul}}}{N_{\mathrm{t}}} \mathbb{E}\left[\sum_{\substack{l=1 \\ l \neq i}}^{K} |\hat{\mathbf{h}}_i^{\mathrm{H}} \mathbf{h}_l|^2\right] + 1} \right\}, \tag{6}$$

where the noise term $\mathbb{E}\left[\hat{\mathbf{h}}_i^{\mathrm{H}} \hat{\mathbf{h}}_i / N_{\mathrm{t}}\right] = 1$. For the downlink,

$$\mathbb{E}[\mathrm{R}_{\mathrm{dl}}] \approx \log_2 \left\{ 1 + \frac{\frac{P_{\mathrm{t}}^{\mathrm{dl}}}{N_{\mathrm{t}}} \mathbb{E}\left[|\mathbf{h}_i \hat{\mathbf{h}}_i^{\mathrm{H}}|^2\right]}{\frac{P_{\mathrm{t}}^{\mathrm{dl}}}{N_{\mathrm{t}}} \mathbb{E}\left[\sum_{\substack{l=1 \\ l \neq i}}^{K} |\mathbf{h}_i \hat{\mathbf{h}}_l^{\mathrm{H}}|^2\right] + 1} \right\}. \tag{7}$$

We now derive the expectation of the signal and interference terms in Sec.III-A and Sec.III-B, respectively.

A. Expected Signal Power

We derive the expected signal power for analog MRC on the uplink in detail, while for the downlink we only give the final result as a similar analysis applies. The expected signal power for the uplink can be derived as follows,

$$\begin{aligned}\mathbb{E}\left[\left|\hat{\mathbf{h}}_i^H\mathbf{h}_i\right|^2\right] &= \mathbb{E}\left[\sum_{j=1}^{N_t}|h_{ij}|^2\right] + \mathbb{E}\left[\sum_{j=1}^{N_t}\sum_{\substack{k=1\\ j\neq k}}^{N_t}|h_{ij}||h_{ik}|\right],\\ &= \sum_{j=1}^{N_t}\beta_{ij} + \sum_{j=1}^{N_t}\sum_{\substack{k=1\\ j\neq k}}^{N_t}\sqrt{\beta_{ij}\beta_{ik}}\mathbb{E}[|v_{ij}||v_{ik}|],\end{aligned} \tag{8}$$

where β_{ij} is the link gain from the i^{th} user to the j^{th} antenna and $h_{ij} = \sqrt{\beta_{ij}}v_{ij}$. In (8), v_{ij} and v_{ik} are two correlated complex Gaussian variables, and can be rewritten as $v_{ij} = r_1\exp(j\theta_1)$ and $v_{ik} = r_2\exp(j\theta_2)$. Thus $|v_{ij}| = r_1$ and $|v_{ik}| = r_2$. From [11, p. 97],

$$\mathbb{E}[r_1r_2] = \frac{\pi}{4\sqrt{(S_{11}S_{22})}}(1-\lambda_{12}^2)_2F_1\left(\frac{3}{2},\frac{3}{2},1;\lambda_{12}^2\right), \tag{9}$$

where ${}_2F_1$ is the Gaussian (or ordinary) hypergeometric function; S_{11} and S_{22} are entries of the inverse covariance matrix, $\mathbf{S}$, of v_{ij} and v_{ik}, where

$$\mathbf{S} = \begin{bmatrix} S_{11} & S_{12}\\ S_{21} & S_{22}\end{bmatrix} = \begin{bmatrix} \frac{1}{1-|\rho|^2} & \frac{-\rho}{1-|\rho|^2}\\ \frac{-\rho^*}{1-|\rho|^2} & \frac{1}{1-|\rho|^2}\end{bmatrix}. \tag{10}$$

Also, $\lambda_{12}^2 = \dfrac{|S_{12}|^2}{S_{11}S_{22}} = |\rho|^2$ and ρ is the correlation between v_{ij} and v_{ik}. Applying this result gives

$$\mathbb{E}[|v_{ij}||v_{ik}|] = \frac{\pi}{4}\left(1-|\rho_{ijk}|^2\right)^2 {}_2F_1\left(\frac{3}{2},\frac{3}{2},1;|\rho_{ijk}|^2\right), \tag{11}$$

where ρ_{ijk} is the jk^{th} entry of $\mathbf{R}_i$. When j and k correspond to different BS groups, there is no correlation, $\rho_{ijk} = 0$, and

$$\mathbb{E}[|v_{ij}||v_{ik}|] = \mathbb{E}[|v_{ij}|]^2 = \Gamma\left(\frac{3}{2}\right)^2. \tag{12}$$

Hence, the final result is,

$$\mathbb{E}\{|\hat{\mathbf{h}}_i^H\mathbf{h}_i|^2\} = \sum_{j=1}^{N_t}\beta_{ij} + \sum_{j=1}^{N_t}\sum_{\substack{k=1\\ j\neq k}}^{N_t}\sqrt{\beta_{ij}\beta_{ik}}\delta_{jk}, \tag{13}$$

where

$$\delta_{jk} = \begin{cases}\Gamma(\frac{3}{2})^2, & j,k\notin B_k\\ \frac{\pi}{4}\left(1-|\rho_{ijk}|^2\right)^2 {}_2F_1\left(\frac{3}{2},\frac{3}{2},1;|\rho_{ijk}|^2\right), & j,k\in B_k\end{cases} \tag{14}$$

and B_k is the set of antennas at the same site as antenna k. The downlink expression for the expected signal power is identical.

B. Expected Interference Power

The interference power for the uplink from the l^{th} user to the i^{th} user can be derived as follows,

$$\begin{aligned}\mathbb{E}\left[|\hat{\mathbf{h}}_i^H\mathbf{h}_l|^2\right] &= \mathbb{E}\left[\hat{\mathbf{h}}_i^H\mathbb{E}\left[\mathbf{R}_l^{\frac{1}{2}}\mathbf{u}_l\mathbf{u}_l^H\mathbf{R}_l^{\frac{1}{2}}\right]\hat{\mathbf{h}}_i\right],\\ &= \mathbb{E}\left[\hat{\mathbf{h}}_i^H\mathbf{R}_l\hat{\mathbf{h}}_i\right],\\ &= \mathbb{E}\left[\sum_{j=1}^{N_t}\sum_{k=1}^{N_t}\frac{h_{ij}^*}{|h_{ij}|}(\mathbf{R}_l)_{kj}\left(\frac{h_{ik}}{|h_{ik}|}\right)\right],\\ &= \sum_{j=1}^{N_t}\sum_{k=1}^{N_t}(\mathbf{R}_l)_{kj}\mathbb{E}\left[\frac{v_{ij}^*}{|v_{ij}|}\frac{v_{ik}}{|v_{ik}|}\right].\end{aligned} \tag{15}$$

Reusing the notation, $v_{ij} = r_1\exp(j\theta_1)$ and $v_{ik} = r_2\exp(j\theta_2)$, we have $\mathbb{E}\left[\frac{v_{ij}^*}{|v_{ij}|}\frac{v_{ik}}{|v_{ik}|}\right] = \mathbb{E}[e^{j(\theta_1-\theta_2)}]$. From [11, p. 100],

$$\mathbb{E}\left\{e^{j(\theta_1-\theta_2)}\right\} = \frac{\pi}{4}\rho(1-\rho^2)_2F_1\left(\frac{3}{2},\frac{3}{2},2;|\rho|^2\right). \tag{16}$$

Thus,

$$\begin{aligned}\mathbb{E}\{|\hat{\mathbf{h}}_i^H\mathbf{h}_l|^2\} &= \sum_{j=1}^{N_t}(\mathbf{R}_l)_{jj} + \sum_{j=1}^{N_t}\sum_{\substack{k=1\\ j\neq k}}^{N_t}(\mathbf{R}_l)_{kj}\frac{\pi}{4}\rho_{ijk}(1-|\rho_{ijk}|^2)\\ &\quad\times {}_2F_1\left(\frac{3}{2},\frac{3}{2},2;|\rho_{ijk}|^2\right),\\ &= \sum_{j=1}^{N_t}\beta_{lj} + \sum_{j=1}^{N_t}\sum_{\substack{k=1\\ j\neq k}}^{N_t}(\mathbf{R}_l)_{kj}\kappa_{ijk}\end{aligned} \tag{17}$$

where

$$\kappa_{ijk} = \begin{cases}0, & j,k\notin B_k\\ \frac{\pi}{4}\rho_{ijk}(1-|\rho_{ijk}|^2)_2F_1(\frac{3}{2},\frac{3}{2},2;|\rho_{ijk}|^2), & j,k\in B_k\end{cases} \tag{18}$$

Similarly, the downlink expected interference power is,

$$\begin{aligned}\mathbb{E}\{|\mathbf{h}_i\hat{\mathbf{h}}_l^H|^2\} &= \sum_{j=1}^{N_t}(\mathbf{R}_i)_{jj} + \sum_{j=1}^{N_t}\sum_{\substack{k=1\\ j\neq k}}^{N_t}(\mathbf{R}_i)_{kj}\frac{\pi}{4}\rho_{ljk}(1-|\rho_{ljk}|^2)\\ &\quad\times{}_2F_1\left(\frac{3}{2},\frac{3}{2},2;|\rho_{ljk}|^2\right),\\ &= \sum_{j=1}^{N_t}\beta_{ij} + \sum_{j=1}^{N_t}\sum_{\substack{k=1\\ j\neq k}}^{N_t}(\mathbf{R}_i)_{kj}\kappa_{lkj}\end{aligned} \tag{19}$$

where

$$\kappa_{lkj} = \begin{cases}0, & j,k\notin B_k,\\ \frac{\pi}{4}\rho_{ljk}(1-|\rho_{ljk}|^2)_2F_1\left(\frac{3}{2},\frac{3}{2},2;|\rho_{ljk}|^2\right), & j,k\in B_k.\end{cases} \tag{20}$$

Thus, substituting (13), (14), (17) and (18) into (3), we obtain the per-user spectral efficiency for the uplink. Similarly substituting (13), (14), (19) and (20) into (5), we obtain the per-user spectral efficiency for the downlink. Not only do (17) and (19) provide the exact value of uplink and downlink interference, they also provide an important insight into MU-MIMO with analog processing. When the users all have the same correlation matrix, then $(\mathbf{R}_l)_{kj}\times\rho_{ijk} = |\rho_{ijk}|^2 > 0$ and $(\mathbf{R}_i)_{kj}\times\rho_{ljk} = |\rho_{ljk}|^2 > 0$, which maximizes the interference in (17) and (19) as all summation terms are positive. Hence, equal correlation matrices is the worst case, as shown in [7] for digital MRC. This is the first demonstration of this property for analog processing.

IV. Numerical Results

In this section, numerical results with the following parameters are presented. Four users each with a single antenna are uniformly located in a circular cell with the radius of 100 meters. The unit-less geometric attenuation is $A = 30$ dB and the reference distance is $d_0 = 1$ meter. The total number of antennas $N_t = 32$; the pathloss exponent $\gamma = 3.5$ and the standard deviation of shadowing $\zeta = 6$ dB. The transmit power P_t is chosen to guarantee that 95% of the time the signal-to-noise-ratio (SNR), defined by the ratio of the received power to the noise power in a single-user single-antenna system, exceeds 0 dB. As our approximations of SINR are accurate for arbitrary correlation models, two popular correlation models are considered. For the exponential correlation model in [12], the correlation matrices required for user i are defined by $(\Sigma_{im})_{rs} = [\rho\exp(j\phi_{im})]^{|r-s|}$. Here, ρ is the common magnitude of the correlation between adjacent antennas and $\phi_{im} \sim U[0, 2\pi]$ is a user specific phase at each antenna group. We also consider the one-ring correlation model [13], with an angle spread of 30° and a central azimuth angle with a uniform distribution within $[0, 2\pi]$ for each user at each antenna group. We refer to this model as *OR.uni*. As LoS will play an important role in upcoming systems, we are also interested in the impact of Rice K factors on the BS layouts. The model for the uplink Ricean channel for the i^{th} user can be written as

$$\mathbf{h}_i = \sqrt{\frac{K_i}{K_i+1}}\bar{\mathbf{u}}_i + \sqrt{\frac{1}{K_i+1}}\mathbf{R}_i^{\frac{1}{2}}\mathbf{u}_i,$$

where K_i is the Rice factor, $\bar{\mathbf{u}}_i$ is the specular (LoS) component and $\mathbf{u}_i$ ($N_\text{t} \times 1$) is the diffuse (scattered) component. $\bar{\mathbf{u}}_i$ ($N_\text{t} \times 1$) is governed by the transmit and receive array response vectors [14]. As we only consider a uniform linear array (ULA) with a single antenna at the receiver, the LoS vector can be written as, $\bar{\mathbf{u}}_i = \mathbf{u}_\text{tx}(\theta_i)$, $\mathbf{u}_\text{tx}(\theta_i) = [1, e^{j2\pi d\cos(\theta_i)}, e^{j2\pi d2\cos(\theta_i)}, ..., e^{j2\pi d(N_\text{t}-1)\cos(\theta_i)}]$, where d is the normalized antenna spacing, assuming to be half the carrier wavelength. Finally, θ_i is the angle of arrival, $\theta_i \sim U[0, 2\pi]$.

Fig.1 illustrates the CDF of the uplink expected per-user spectral efficiency based on the *Dis4* system architecture with three different correlation models. The expectation is computed over the fast-fading and the CDF depicts the impact of the variations in large-scale fading link gains. *Exp.0.95fixed* denotes the exponential correlation model with a fixed correlation coefficient $\rho = 0.95$ and no random phase; *OR.uni* denotes the one-ring correlation model; *Exp0.7random* denotes the exponential correlation with uniformly distributed phase on $[0, 2\pi]$ and $\rho = 0.7$. In this figure we compare the CDF of the derived analog per-user spectral efficiency approximation with its simulated counterparts. As we can see, the derived approximations are tight for all three correlation models considered.

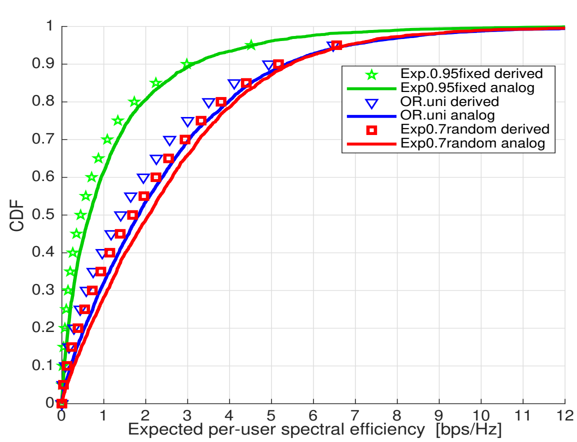

Fig. 1: Expected per-user spectral efficiency CDFs of analog MRC for an uplink *Dis4* system with three correlation models

In Fig.2 we present the performance comparison of analog and digital MRC for three system layouts: *Cen, Dis2, Dis4*. Using the same propagation parameters as in Fig.1 and the *OR.uni* correlation model, the CDFs of per-user spectral efficiency are shown. Generally, digital MRC outperforms analog MRC in all three systems. This is mainly due to the fact that analog MRC is incapable of changing the amplitude of the incoming signals. For digital MRC, the system benefits from greater antenna distribution. However, the trend is opposite for analog MRC, where *Dis2* and *Cen* have almost the same performance and both outperform *Dis4*. Digital MRC benefits from a more distributed system where there is a higher probability of a strong link gain to one of the antenna clusters. Analog MRC, however, is not able to benefit the users by optimising the receive SNR over different link gains. Thus the centralized system results in the strongest signal power compared with distributed systems when adopting analog MRC processing.

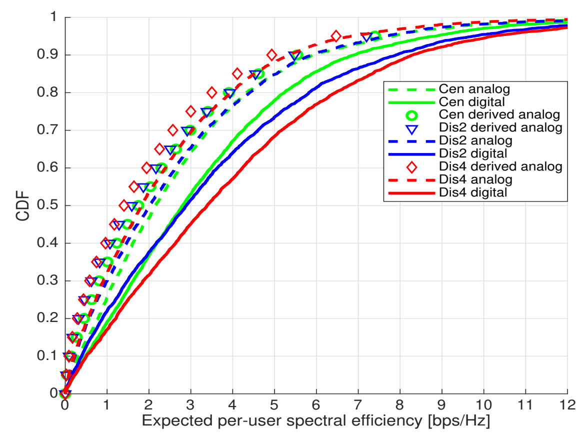

Fig. 2: Performance comparison of expected per-user spectral efficiency CDFs between analog and digital MRC for uplink

We show numerical results for the Ricean channels for the *Cen* and *Dis4* systems in Fig.3 and Fig.4, respectively. We provide simulations rather than an exact analysis as it has been shown [15] that the required results for the Ricean case involve a doubly infinite sum of hyper-geometric functions, which has only a limited advantage over simulation. The trends in Fig.3 and Fig.4 illustrate that increasing the Rice K factors can actually increase per-user spectral efficiency in both *Cen* and *Dis4* systems as LoS reduces channel fading fluctuations and also the MRC inter-user-interference as shown in [5]. The gap between analog and digital MRC diminishes to zero in a *Cen* system when the Rice K is greater than 5 dB, where the strong LoS results in low diversity of signals for which analog and digital MRC have almost the same performance. This is not the case for the *Dis4* system due to the link gain diversity from which digital MRC benefits.

This article has been accepted for publication in a future issue of this journal, but has not been fully edited. Content may change prior to final publication. Citation information: DOI 10.1109/TVT.2018.2885555, IEEE Transactions on Vehicular Technology

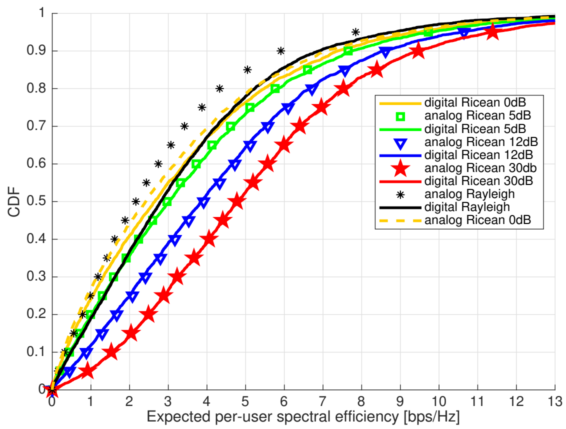

Fig. 3: Expected per-user spectral efficiency CDFs of analog and digital MRC for an uplink *Cen* system

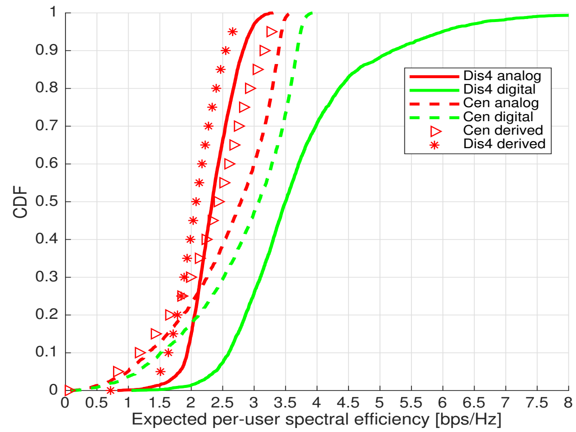

Fig. 5: Expected per-user spectral efficiency CDFs of analog and digital MRC for downlink *Dis4* and *Cen* systems

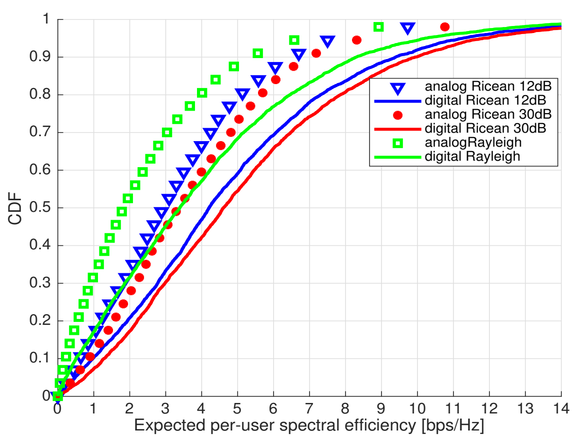

Fig. 4: Expected per-user spectral efficiency CDFs of analog and digital MRC for an uplink *Dis4* system

Finally, in Fig.5 we consider the downlink system. The figure not only shows the accuracy of the approximations, but also that digital MF in *Dis4* significantly outperforms the *Cen* system. This is mainly due to the high diversity of link gains in a distributed system as the per-user spectral efficiency is affected by the desired user's link gains at different sites. Examining the derivations of (13) and (19), both the numerator and denominator of the derived SINR for the downlink are affected by the same desired user's link gain, $\bar{\beta}_{im}$, which is the same for both the numerator and denominator in the centralized system. Dividing by $\bar{\beta}_{im}$ for both the numerator and denominator in (5), we see that variations in the CDF of the expected per-user SINR are limited, reflected in Fig.5 by the steep curves of the *Cen* system. On the other hand, in the distributed system $\bar{\beta}_{im}$ takes on different values for the numerator and denominator of the SINR, leading to more diversity in the *Dis4* system for digital MRC.

V. Conclusion

We have derived closed-form approximations to the SINR for analog MRC/MF for uplink/downlink systems, leading to an insightful comparison of analog and digital processing for three different BS layouts. While digital MRC benefits from increased BS decentralization, the same does not hold for analog MRC. We presented an analysis of the impact of different Rice K factors on both centralized and distributed systems. When increasing the K factor in a centralized system, the performance of analog MRC approaches that of digital MRC, while the performance gap between the two technique remains in a distributed system.

References

[1] M. K. Karakayali, G. J. Foschini, and R. A. Valenzuela, "Network coordination for spectrally efficient communications in cellular systems," *IEEE Wireless Commun.*, vol. 13, no. 4, pp. 56–61, 2006.

[2] K. T. Truong and R. W. Heath, "The viability of distributed antennas for massive MIMO systems," in *Signals, Systems and Computers, 2013 Asilomar Conference on*. IEEE, 2013, pp. 1318–1323.

[3] T. Eng, N. Kong, and L. B. Milstein, "Comparison of diversity combining techniques for Rayleigh-fading channels," *IEEE Trans. Commun.*, vol. 44, no. 9, pp. 1117–1129, 1996.

[4] P. O. Akuon and H. Xu, "Optimal error analysis of receive diversity schemes on arbitrarily correlated Rayleigh fading channels," *IET Communications*, vol. 10, no. 7, pp. 854–861, 2016.

[5] Q. Zhang, S. Jin, K.-K. Wong, H. Zhu, and M. Matthaiou, "Power scaling of uplink massive MIMO systems with arbitrary-rank channel means," *IEEE J. Sel. Topics Signal Process.*, vol. 8, no. 5, pp. 966–981, 2014.

[6] R. H. Louie, M. R. McKay, and I. B. Collings, "Maximum sum-rate of MIMO multiuser scheduling with linear receivers," *IEEE Trans. Commun.*, vol. 57, no. 11, 2009.

[7] H. Tataria, P. J. Smith, L. J. Greenstein, P. A. Dmochowski, and M. Matthaiou, "Impact of line-of-sight and unequal spatial correlation on uplink MU-MIMO systems," *IEEE Wireless Commun. Lett.*, vol. 6, no. 5, pp. 634–637, 2017.

[8] M. Kang and M.-S. Alouini, "Largest eigenvalue of complex Wishart matrices and performance analysis of MIMO MRC systems," *IEEE J. Sel. Areas Commun*, vol. 21, no. 3, pp. 418–426, 2003.

[9] C. Kong, C. Zhong, M. Matthaiou, and Z. Zhang, "Performance of downlink massive MIMO in Ricean fading channels with ZF precoder," in *Communications (ICC), 2015 IEEE International Conference on*. IEEE, 2015, pp. 1776–1782.

[10] W. Tan, S. Jin, J. Wang, and M. Matthaiou, "Achievable sum-rate of multiuser massive MIMO downlink in Ricean fading channels," in *Communications (ICC), 2015 IEEE International Conference on*. IEEE, 2015, pp. 1453–1458.

[11] K. S. Miller, *Complex Stochastic Processes: An Introduction to Theory and Application*. Advanced Book Program, 1974.

[12] B. Clerckx, G. Kim, and S. Kim, "Correlated fading in broadcast MIMO channels: Curse or blessing?" in *Global Telecommunications Conference, 2008. IEEE GLOBECOM 2008.* IEEE, 2008, pp. 1–5.

[13] D.-S. Shiu, G. J. Foschini, M. J. Gans, and J. M. Kahn, "Fading correlation and its effect on the capacity of multielement antenna systems," *IEEE Trans. Commun.*, vol. 48, no. 3, pp. 502–513, 2000.

[14] M. R. Akdeniz, Y. Liu, M. K. Samimi, S. Sun, S. Rangan, T. S. Rappaport, and E. Erkip, "Millimeter wave channel modeling and cellular capacity evaluation," *IEEE J. Sel. Areas Commun.*, vol. 32, no. 6, pp. 1164–1179, 2014.

[15] J. R. Mendes and M. D. Yacoub, "A general bivariate Ricean model and its statistics," *IEEE Trans. Veh. Technol.*, vol. 56, no. 2, pp. 404–415, 2007.